Journal of Materials Chemistry C

PAPER

Cite this: J. Mater. Chem. C, 2014, 2, 4552

Non-classical donor–acceptor–donor chromophores. A strategy for high two-photon brightness†

Adina I. Ciuciu,[a] Dikhi Firmansyah,[b] Vincent Hugues,[c] Mireille Blanchard-Desce,*[c] Daniel T. Gryko*[bd] and Lucia Flamigni*[a]

Received 5th February 2014
Accepted 10th March 2014

DOI: 10.1039/c4tc00234b

www.rsc.org/MaterialsC

Rod-like π-expanded bis-imidazo[1,2-*a*]pyridines were designed and synthesized. Strategic placement of a central electron-poor unit at position C3 of the imidazo[1,2-*a*]pyridine core resulted in donor–acceptor–donor quadrupolar systems. We further demonstrated the applicability of the Ortoleva–King–Chichibabin tandem process in the preparation of complex imidazo[1,2-*a*]pyridines. The monomer model heterocycles, differing by substitution at C2 and C3, displayed luminescence properties marginally dependent on the substitution pattern and conjugation extension. The highest luminescence quantum yield (ϕ_{fl} *ca.* 0.2) is shown by the model compounds without a substitution at C3, whereas lower values are measured for the others. Quantum yields in toluene for the quadrupolar systems varied from ϕ_{fl} = 0.7 to ϕ_{fl} > 0.9. Apart from bis-imidazo[1,2-*a*]pyridine possessing two methyl groups, with ϕ_{fl} = 0.69 in toluene and 0.35 in dichloromethane, the luminescence properties were only slightly affected by the change in the solvent. Most of the fluorescence lifetimes ranged from 1–2 ns and the radiative rate constants reached values of *ca.* 6 × 10^8 s^{-1}. Intense phosphorescence spectra at 77 K with lifetimes in the second range (τ = 0.6–1.3 s) are recorded for the monomers, whereas for the bis-imidazo[1,2-*a*]-pyridines, phosphorescence spectra are detected only after enhancing intersystem crossing by heavy atoms. Non-linear optical properties of bis-imidazo[1,2-*a*]pyridines revealed two-photon absorption cross-sections (σ_2) typically of the order of 500–800 GM. The remarkable fluorescence quantum yield, in combination with high a two-photon absorption cross-section, generated a two-photon brightness of ~500 to 750 GM units within the biological window (700–800 nm).

Introduction

Two-photon excited fluorescence (TPEF) imaging has attracted much interest for biological applications because of the intrinsic three-dimensional resolution it offers and since the use of NIR laser excitation light allows the advantages of minimal background auto-fluorescence, deep light penetration, and minimal photodamage to living organisms.[1] Thus, the development of high-performance TPEF bio-probes is an expanding field of investigation, particularly for the synthesis of compounds with large values of two-photon brightness (*i.e.* $\phi_{fl} \times \sigma_2$, where ϕ_{fl} is the fluorescence quantum yield and σ_2 is the two-photon absorption cross-section). The contribution of dipolar and quadrupolar architectures to achieve high σ_2 has driven the efforts to prepare two photon probes that incorporate various electron-donating and electron-withdrawing moieties into their structures.[2]

Since the identification of two-photon excited fluorophores is key to the field of bioimaging, we turned our attention towards imidazo[1,2-*a*]pyridine scaffolds for the construction of donor–acceptor–donor (D–A–D) quadrupolar systems. These compounds are particularly attractive because they are electron-rich aromatic heterocycles possessing inherently high fluorescence quantum yields. We envisioned the construction of quadrupolar compounds bearing a central electron-withdrawing unit combined with two electron-rich imidazo[1,2-*a*]-pyridines that would afford materials possessing both high fluorescence quantum yield and large two-photon absorption cross-section.[3] In addition to their interesting luminescence properties[4] and the advances in their synthesis,[5] imidazo[1,2-*a*]-pyridines show well-known biological activities.[6] These drug-like scaffolds hold great promise for the design of fluorescence probes for *in vivo* imaging because these molecules can

[a]*Istituto per la Sintesi Organica e Fotoreattivita' (ISOF), CNR, Via P. Gobetti 101, 40129 Bologna, Italy. E-mail: lucia.flamigni@isof.cnr.it; Fax: +39 (0)51 639 98 44; Tel: +39 (0)51 639 98 12*

[b]*Warsaw University of Technology, Noakowskiego 3, 00-664, Warsaw, Poland. Fax: +48 22 628 27 41; Tel: +48 22 234 58 01*

[c]*Université de Bordeaux, ISM (UMR5255 CNRS), F 33400, Bordeaux, France. E-mail: mireille.blanchard-desce@iu-bordeaux.fr*

[d]*Institute of Organic Chemistry Polish Academy of Sciences, Kasprzaka 44/52 01-224, Warsaw, Poland. E-mail: dtgryko@icho.edu.pl; Fax: +48 22 632 66 81; Tel: +48 22 343 30 63*

† Electronic supplementary information (ESI) available. See DOI: 10.1039/c4tc00234b

potentially retain their molecular recognition ability and thereby can be used as specific probes to target biologically relevant dedicated sites.

The fluorescence properties of imidazo[1,2-*a*]pyridines may be enhanced by altering the emission quantum yield and the Stokes shift as well as by tuning their emission wavelength. Optimization of these factors will improve their usefulness in fluorescence microscopy and also for optical materials. Therefore, we have explored the possibility of altering the patterns of substituents on the imidazo[1,2-*a*]pyridine scaffold. Several studies on imidazo[1,2-*a*]pyridines have taken advantage of the excited state intramolecular proton transfer (ESIPT)[4b,c] process, both in solution and in the solid state.[4d,4g,7] Although interesting luminescence properties of imidazo[1,2-*a*]pyridine derivatives have been presented, quantitative data of fluorescence quantum yields have not been reported.[8]

To date, only limited success has been achieved in optimizing the luminescence properties of imidazo[1,2-*a*]pyridines, particularly in polar solvents. A recent report based on combinatorial synthesis and screening showed that a derivative of the imidazo [1,2-*a*]pyridine drug Zolpidem can lead to luminescence quantum yields ranging from $\phi_{fl} = 0.11$ to $\phi_{fl} = 0.89$ in dimethylsulfoxide solutions.[9] Substitution at the C2 position proved to be a valid strategy for increasing the luminescence quantum yield. A $\phi_{fl} = 0.83$ in ethanol solutions was obtained by substitution with long chain arylpiperazines.[10] We[3] and others[4c] have reported that introduction of various aryl substituents at C2 of imidazo[1,2-*a*]-pyridines improved their luminescence properties up to $\phi_{fl} = 0.7$–0.8. Substitution on the six membered ring was less effective on the fluorescence properties, whereas extension of the delocalization increased the luminescence quantum yields in toluene solutions.[3]

Some preliminary experimental results on non-linear second harmonic generation properties of chromophores involving imidazo[1,2-*a*]pyridines have been described in the literature.[11] Later, we reported[3] the first quadrupolar systems which contained two imidazo[1,2-*a*]pyridines moieties connected by one electron withdrawing unit. These compounds displayed reasonable fluorescence yields of $\phi_{fl} = 0.3$ in toluene and σ_2 of the order of 10^2 GM.

The aim of this study was to increase both ϕ_{fl} and σ_2 in quadrupolar systems based on imidazo[1,2-*a*]pyridines. Imidazo-[1,2-*a*]pyridines possess the highest electron-density at C3 and this is usually the site of attack in electrophilic aromatic substitution.[4b,12] We envisioned that attaching the acceptor core at the C3 position would lead to compounds with favorable optical properties. Herein, we report the synthesis, spectroscopic and photophysical properties, as well as the two-photon absorption characteristics of a series of compounds comprising five quadrupolar structures formed by two differently substituted imidazo [1,2-*a*]pyridine moieties (D) connected by either a pyrazine or a 1,4-dicyano benzene group (A) to construct a D–A–D structure.

Results and discussion

Design and synthesis

We hypothesized that attachment of an electron-acceptor to the most electron-rich position of the imidazo[1,2-*a*]pyridine would significantly improve the charge transfer character of the quadrupolar molecules, resulting in high two-photon absorption cross-section values. Based on our previous experience with imidazo[1,2-*a*]pyridines, we chose 2-amino-5-(trifluoromethyl)-pyridine (**1**) as the backbone. Since the trifluoromethyl group is moderately electron-withdrawing, we expected an improved stability of the final dye. Unlike nitrile groups, which could decrease the solubility or nitro and carbonyl groups which may quench the fluorescence, CF_3 groups have limited effects on the optical properties.

Three imidazo[1,2-*a*]pyridines were synthesized as the starting materials (Schemes 1 and 2). Compound **3a** was synthesized following known procedures for condensation of amine **1** and chloroacetone (**2a**).[13] Using the tandem Ortoleva–King–Chichibabin method,[7a] we obtained compound **3b** in almost 90% yield, while analogous **3c** was obtained in a moderate yield of 44%. The triethylene glycol group was introduced to improve the solubility of the final dyes in more polar solvents.

Imidazo[1,2-*a*]pyridines **3a–c** were easily converted into bromo-derivatives **4a–c** using well established general procedures.[12b,d,g] The bromination took place at room temperature and the product precipitated upon completion of the reaction. Consequently, products **4a–c**, were pure enough and were obtained in high yields. The terminal alkynes **6a–c** were prepared following a typical pathway, *i.e.*, the Sonogashira reaction with 2-methylbut-3-yn-2-ol, to obtain the alkynols **5a–c**

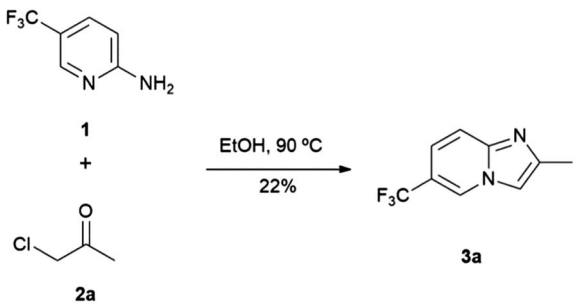

Scheme 1 Synthesis of imidazo[1,2-*a*]pyridine **3a**.

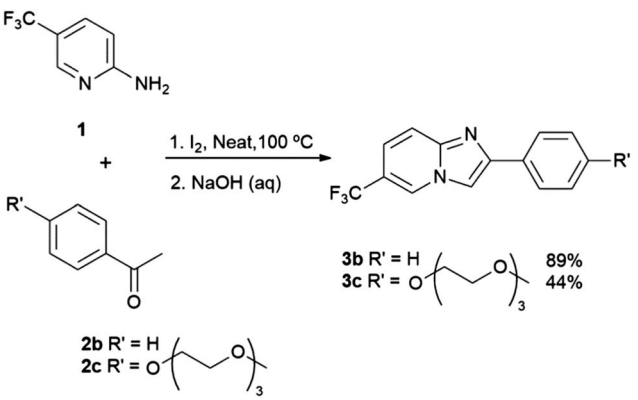

Scheme 2 Synthesis of imidazo[1,2-*a*]pyridines.

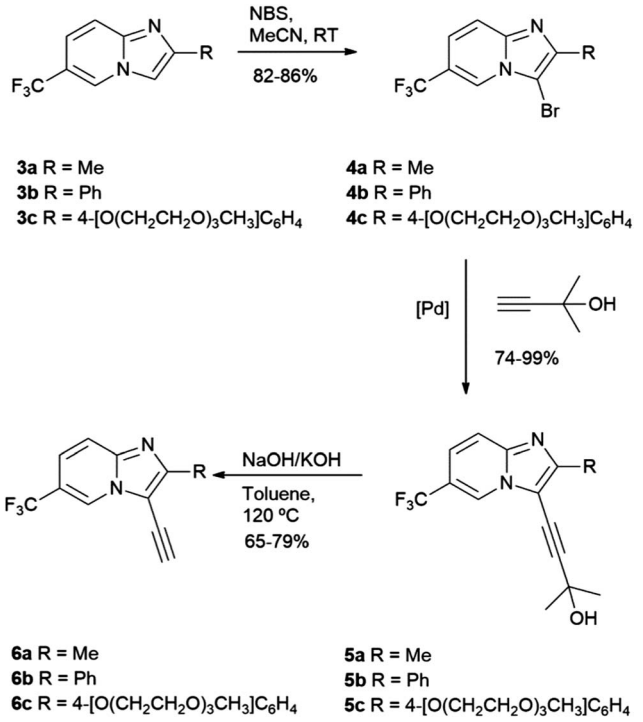

Scheme 3 Preparation of terminal alkynes.

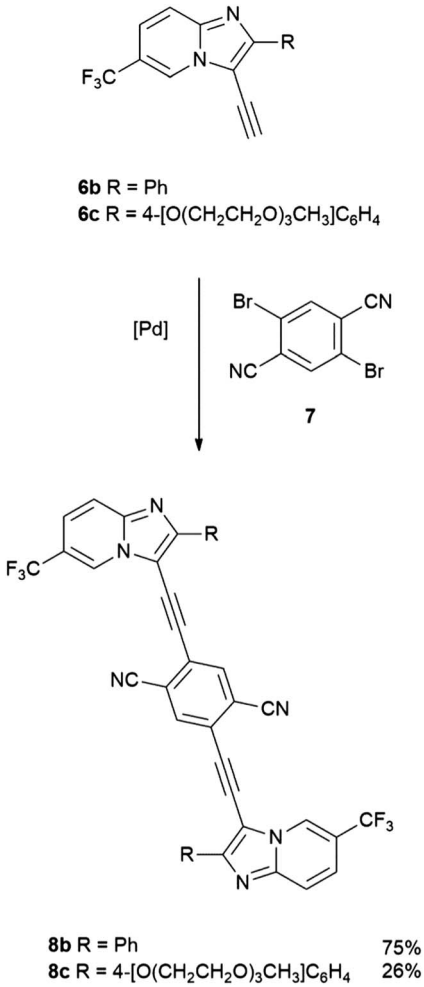

Scheme 4 Synthesis of D–A–D systems possessing the terephthalonitrile core.

followed by deprotection under basic conditions (Scheme 3). Although the removal of the protecting group required extremely dry toluene and harsher conditions compared to silyl-based protecting groups, the clear advantage was the substantial polarity difference between products and substrates.[14] This polarity difference facilitated the removal of the unreacted starting material during the purification process.

Initially, 2,5-dibromoterephthalonitrile (7) was used as the starting material for the final double Sonogashira coupling (Scheme 4). Compound 7 was a very reactive starting material for Sonogashira coupling, and the addition of CuI (as co-catalyst) could often be omitted. It is worth noting that Sonogashira coupling without CuI was very favorable, since the formation of the Glaser coupling by-product had ceased. Following this procedure, D–A–D quadrupoles **8b** and **8c** were synthesized in high yields.

The phenyl substituted imidazo[1,2-*a*]pyridine **6b** was transformed into product **8b** in 75% yield, making the overall yield for this five steps process ~40%. Because dye **8b** was poorly soluble, we undertook the synthesis of its analogue **8c**. The double Sonogashira reaction starting from substrate **6c** yielded quadrupole **8c** in only a moderate yield. The presence of a larger substituent on alkynes tends to make the coupling more difficult due to steric effects. On the other hand, dye **8c** possessed far better solubility compared to **8b**, including in DMSO.

Pd-catalyzed coupling at high temperature is known to lead to debromination of products. Attempts to improve the yield by reducing the temperature and prolonging the reaction time were not successful for **8c**. As verified by ^{1}H NMR, a part of the reactant was transformed into the mono-substituted product. In the case of bis-imidazo[1,2-*a*]pyridines, the product is usually well soluble in dichloromethane and $CHCl_3$ and poorly soluble in hexane/EtOAc. Purification was based on the latter's solubility property and impurities were removed by trituration.

Pyrazine was chosen as an alternative electron-withdrawing core. 2-Bromo-5-iodopyrazine (**9**), the key building block, was synthesized *via* a known procedure.[15] Electron-deficiency of compound **9** facilitated the Sonogashira coupling without CuI. We observed a decrease in yield as the size of the substituent increased. This result was consistent with the previous results for compounds **8b** and **8c**. Steric hindrance also affected the temperature required for reactivity of imidazo[1,2-*a*]pyridines. Reactions with smaller substituents usually required lower temperatures to reach completion than did reactions with larger substituents (Scheme 5). Pyrazine derivatives **10a–c** displayed better solubility in $CHCl_3$ compared to **8b–c**, which can be attributed to the two electron pairs present in their cores. All synthesized quadrupoles demonstrated high thermal resistance despite their low solubility. Decomposition only occurred at a temperature above 240 °C.

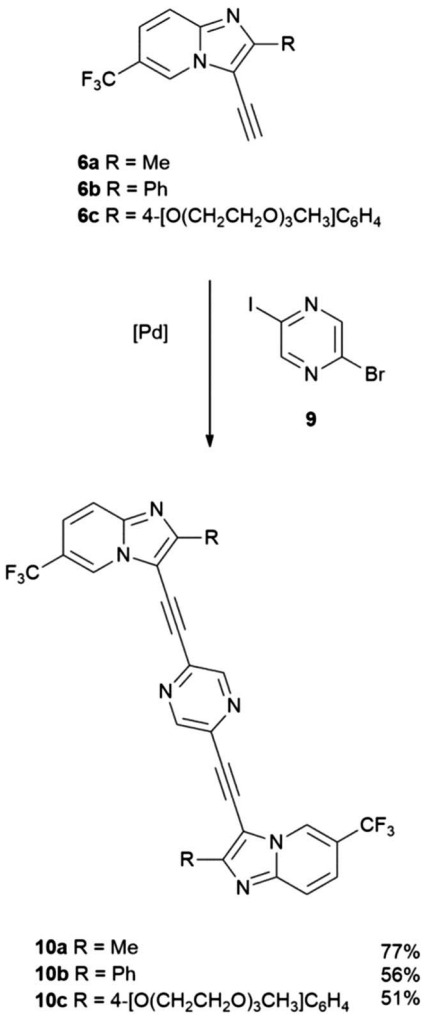

Scheme 5 Synthesis of D–A–D systems possessing a pyrazine core.

Linear optical properties

Absorption. Chart 1 shows the structures of the investigated compounds. Prior to construction of the dimeric structures, we prepared 3 monomers for every dimer, each with a different substituent chosen to maximize the properties of solubility and photo or thermal stability. Family **3a–c** had no substituent at C3, family **5a–c** had a tertiary alcohol linked to an alkyne group, and family **6a–c** displayed an alkyne group.

Monomers **6a–c** exhibited excellent stability in toluene both under light and in the dark, whereas monomers **3a–c** and in particular **5a–c** were less stable under prolonged (3–20 hours) irradiation under laboratory light. Bis-imidazo[1,2-*a*]pyridines **10a–c** and **8b,c** in toluene proved non perfectly stable after a few hours of light exposure. In dichloromethane, all monomeric samples as well as the corresponding bis-imidazo[1,2-*a*]pyridines **10a–c** and **8b,c** showed excellent photo and thermal stability over hours or days. The photophysical properties of the samples **8b,c** and **10a–c** were examined in two solvents of different polarities, toluene (TOL, $\varepsilon = 2.38$) and dichloromethane (DCM, $\varepsilon = 8.9$) and compared to those of the individual imidazopyridine components **3a–c**, **5a–c** and **6a–c**.

The absorption spectra determined in TOL for the samples are illustrated in Fig. 1 (spectra determined in DCM are presented in Fig. S1, ESI section†) and data are collected in Table 1. Compounds **3a–c**, without substitution at C3, displayed a single broad band with a maximum at 320–340 nm. The intensity of this band increased as the units intended to link the monomer to the core structure were extended and the λ_{max} become slightly more red-shifted (from 320 nm to 340 nm). The monomers **5a–c** and **6a–c** displayed similar absorption spectra with a structured band around 300 nm and a broader one at 340–360 nm. The absorption spectra of the bis-imidazo[1,2-*a*]pyridines were characterized by an intense band containing a shallow vibrational structure at 480–490 nm for the 1,4-dicyanobenzene-containing bis-imidazo[1,2-*a*]pyridines **8b,c** and at 420–460 nm for the structures possessing a pyrazine bridge, **10a–c**. The absorption spectra of the bis-imidazo[1,2-*a*]pyridines were distinctly different from those of the component monomers, which is a clear indication of an extended electronic delocalization in the quadrupolar structures. The molar absorption coefficients determined in TOL and DCM were almost identical (Table 1). The low solubility of **8b** prevented a careful determination of the molar absorption coefficient. Therefore the absorption spectrum of **8b** was normalized to that of the similar compound **8c**. For the spectra acquired in the more polar DCM, we observed a hypsochromic shift of a few nanometers (2–4 for monomers, 6–9 for bis-imidazo[1,2-*a*]pyridines) as compared to spectra in TOL (Table 1).

Emission. The emission spectra of monomers **3a–c**, **5a–c** and **6a–c** were acquired using 325 nm as the excitation wavelength. The fluorescence quantum yields were determined using quinine sulfate as a standard. The emission spectra in TOL, presented in Fig. 2, showed emission maxima in the 380–420 nm region and displayed good mirror images with the absorption spectra. The **a** series, with a methyl substituent at position 2 of imidazo[1,2-*a*]pyridine, manifested the lowest emission quantum yield ($\phi_{fl} = 0.06$–0.17) whereas the **c** series, characterized by a 4-(oligoethyleneglycol)phenyl (OTEG) substituent in the same position produced the highest yield (0.17–0.23), Table 1. Within each **a**, **b**, and **c** series, the **3** family with no substituent at C3 exhibited the highest emission quantum yields, ranging from 0.17 to 0.23. As expected, compounds **5** and **6** of each series, differing only for the presence of a tertiary alcohol at the alkyne substituent, have almost the same properties (Table 1). The emission spectra of monomers in DCM are displayed in Fig. S2, ESI† section and the corresponding data are collected on Table 1. The band maxima and emission quantum yield of each dye were unaffected by the solvent polarity, within experimental error.

Fluorescence lifetimes of 1–2 ns were determined for the entire library of compounds, (with the exception of sample **3a** which had a $\tau > 6$ ns) and found to be independent of solvent polarity (Table 1). A k_{rad} ($k_{rad} = \phi_{fl}/\tau$) in the order of 10^7 to 10^8 s^{-1} was calculated for the monomers. The measured lifetimes are in agreement with those of similar imidazole-based compounds reported in the literature.[3,7b,16] The emitting singlet states were tentatively identified as π–π^* in nature, as based on the molar absorption coefficients of the corresponding

R^1	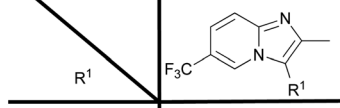	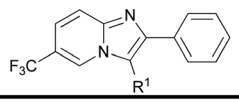	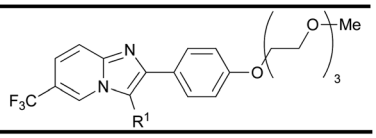
H	**3a**	**3b**	**3c**
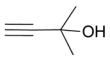	**5a**	**5b**	**5c**
	**6a**	**6b**	**6c**

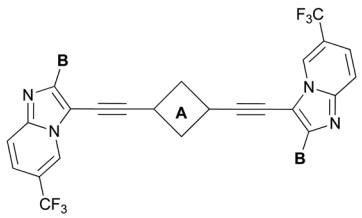

A	B		
	CH_3		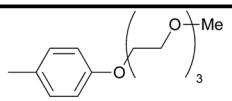
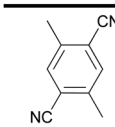	**10a**	**10b**	**10c**
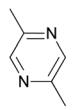		**8b**	**8c**

Chart 1 Structures of the investigated compounds.

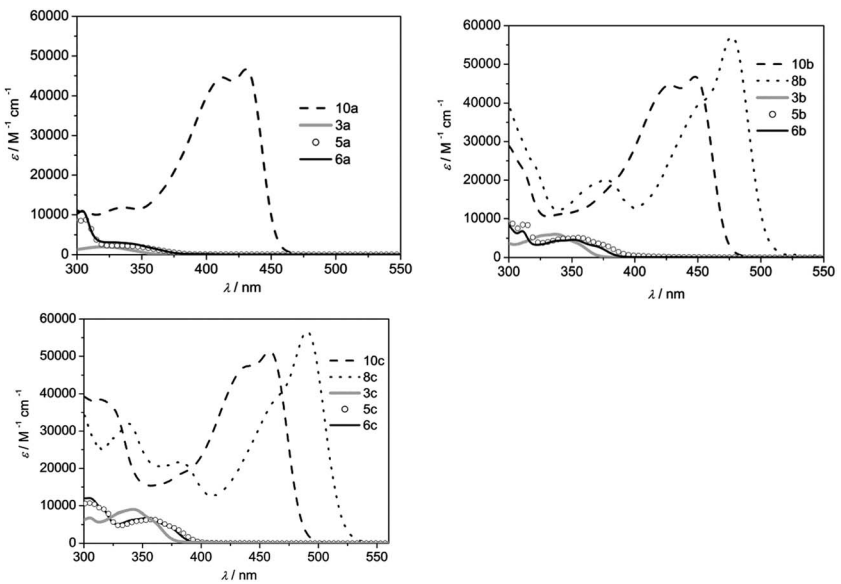

Fig. 1 Absorption spectra of the studied compounds in TOL solutions.

Table 1 Photophysical parameters in TOL and DCM measured at 295 K. Monomers are in italics

	TOL				DCM			
	$\varepsilon^{max}/M^{-1}\ cm^{-1}$ (λ_{max}/nm)	λ_{em}^{max}/nm	ϕ_{fl}	τ/ns	$\varepsilon^{max}/M^{-1}\ cm^{-1}$ (λ_{max}/nm)	λ_{em}^{max}/nm	ϕ_{fl}	τ/ns
3a	2000 (320)	402	0.17	6.33	2400 (317)	400	0.20	6.56
5a	8800 (306)	423	0.06	3.20	9500 (304)	422	0.07	3.16
	2300 (333)				2500 (330)			
6a	11 000 (304)	419	0.06	2.91	8700 (302)	418	0.07	2.80
	3100 (331)				2500 (327)			
10a	11 800 (335)	455; 477	0.69	1.38	13 000 (330)	470; 490	0.35	1.35
	44 600 (412)				46 700 (410)			
	46 600 (431)				47 000 (424)			
3b	5700 (327)	379; 401; 416	0.18	2.40	6300 (324)	374; 394; 415	0.19	2.15
	6000 (338)				6500 (333)			
	3700 (354)				4000 (350)			
5b	9000 (313)	401; 423; 444	0.13	2.63	9500 (311)	400; 420; 442	0.13	2.48
	4900 (343)				5000 (340)			
	5100 (356)				5100 (352)			
	3400 (374)				3100 (371)			
6b	6800 (311)	396; 416; 440	0.15	2.86	7200 (309)	394; 413; 433	0.15	2.67
	4300 (338)				4800 (336)			
	4600 (351)				5000 (348)			
	3000 (368)				3000 (367)			
8b	n.d.	507; 541	0.92	2.31	n.d.	507; 540	0.83	2.66
10b	44 700 (428)	473; 500	0.93	1.49	48 400 (423)	480; 503	0.88	1.81
	46 700 (448)				47 800 (440)			
3c	8000 (329)	385; 402; 417	0.23	2.24	8300 (324)	384; 403; 416	0.24	1.98
	9000 (342)				9500 (336)			
	6200 (358)				6400 (354)			
5c	10 700 (305)	408; 426; 448	0.17	2.55	10 900 (303)	405; 424; 446	0.18	2.41
	5900 (345)				6400 (343)			
	6400 (359)				6700 (355)			
	3900 (379)				3900 (376)			
6c	12 000 (305)	399; 420; 438	0.19	2.75	11 800 (303)	398; 419; 436	0.19	2.54
	6300 (342)				6900 (338)			
	6900 (355)				7300 (351)			
	4700 (371)				4800 (370)			
8c	32 000 (339)	525; 562	0.84	2.67	32 800 (333)	529; 563	0.80	3.25
	21 800 (384)				23 200 (381)			
	38 100 (462)				40 100 (459)			
	56 700 (490)				55 700 (484)			
10c	38 100 (318)	489; 517	0.87	1.73	40 000 (310)	498; 525	0.82	2.27
	47 300 (439)				45 800 (432)			
	51 300 (459)				46 800 (450)			

absorption bands, on the lack of effect of solvent polarity on the energy and quantum yields of the fluorescence emission, and on the large emission values.

The bis-imidazo[1,2-*a*]pyridines **10a–c** and **8b,c** were excited at 424 nm and the emission quantum yields were measured using coumarin 153 as the reference compound. The results are summarized in Table 1 for both solvents and the spectra in TOL are shown in Fig. 3. Fig. S3 (ESI†) shows the spectra of the dimeric structures in DCM. The emission bands were located at 470–520 nm for the bis-imidazo[1,2-*a*]pyridines containing the pyrazine unit and at 510–570 for bis-imidazo[1,2-*a*]pyridines containing the dicyanobenzene unit. The emission quantum yields were extremely high, up to 0.93 (Table 1). The emission spectra displayed a good mirror image with the absorption spectra, reproducing the vibrational structures and, as in the assignment for the monomers, the fluorescence was ascribed to the transition from the lowest π–π* singlet excited state. A closer examination of the spectra in more polar solvents revealed the effects of charge transfer (CT). The spectra measured in the more polar DCM were broader and the luminescence quantum yield lower, but generally by less than 10%. The exception is for the less substituted **10a** structure, which displayed a 50% decrease in the emission quantum yield from TOL to DCM (Table 1). In the case of samples **10a–c** (containing pyrazine) a slight bathochromic shift occurred in DCM, a confirmation of some intramolecular CT character. The extended conjugation in the other bis-imidazo[1,2-*a*]pyridines **8b,c** stabilized the π–π* excited state and weakened the CT character, making their luminescence less affected by the solvent polarity (Table 1). Within the same solvent, a

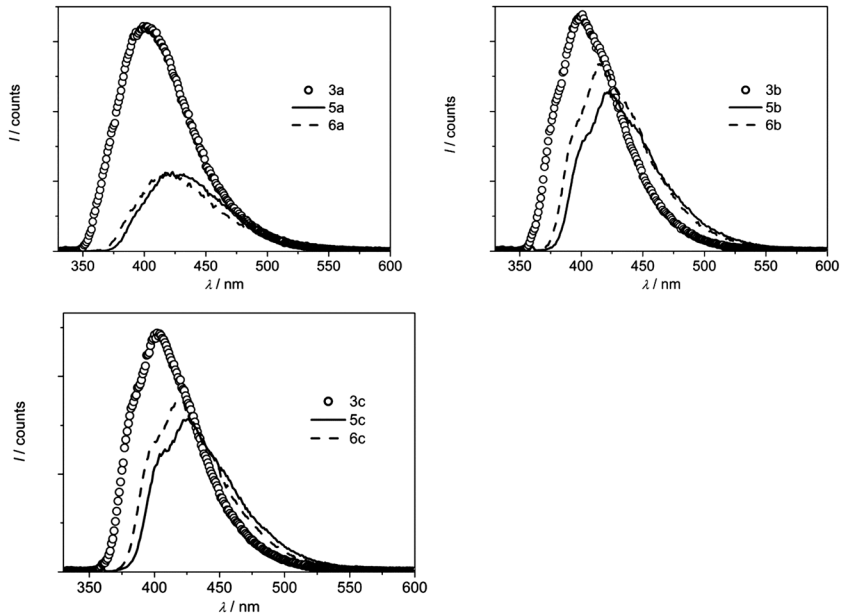

Fig. 2 Fluorescence spectra of optically matched solutions of reference monomers in TOL at room temperature. Excitation wavelength was 325 nm and $A_{325\ nm} = 0.07$.

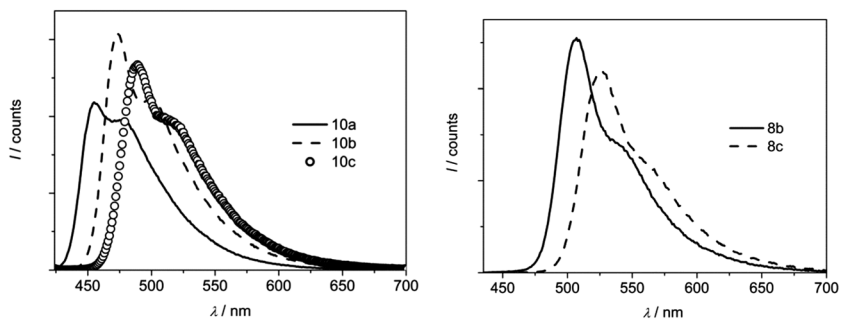

Fig. 3 Fluorescence spectra of optically matched solutions of the bis-imidazo[1,2-*a*]pyridines **10a–c** and **8b,c** in TOL at room temperature. Excitation wavelength was 424 nm and $A_{424\ nm} = 0.07$ for **10a–c** and $A_{424\ nm} = 0.03$ for **8b,c**.

bathochromic shift as the size of the substituent increased from series **a** to **b** and **c**, was evident. The fluorescence lifetimes ranged from 1 to 3 ns (Fig. 4) leading to a calculated $k_{rad} > 10^8$ s^{-1}. To the best of our knowledge, the present samples are the first to exhibit such remarkable luminescence properties for quadrupolar systems based on imidazo[1,2-*a*]pyridine. Excitation spectra in TOL and DCM measured at the emission maxima of both monomers and bis-imidazo[1,2-*a*]pyridines were perfectly superimposable on the corresponding absorption spectra, Fig. S4,† indicating a genuine emission from the lowest excited state and the absence of contaminants.

Compounds **8c** and **10c** could also be dissolved in dimethyl sulfoxide (DMSO) and pure water thanks to the presence of the OTEG side chain. Interestingly, in these environments, the emission is significantly red-shifted (with emission maxima located at 655 nm and 556 nm in H_2O for compounds **8c** and **10c** respectively). This is indicative of significant symmetry breaking and related charge transfer in the excited state (as already reported in more conventional quadrupoles).[17]

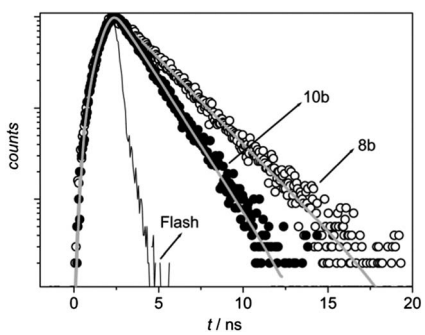

Fig. 4 Fluorescence decay data of **8b** and **10b** together with the corresponding fitting curve (grey) and the excitation profile, in TOL.

Consequently, their fluorescence quantum yield decreases in those polar environments (see Table S1†), leading to a fluorescence quantum yield of 13% for the more hydrophilic dye **10c** in pure water and of 4% for **8c**.

Emission in solid matrices at 77 K. For insight into the behavior of the samples in solid matrices, we performed steady state and time resolved experiments in a solid TOL matrix at 77 K. This experiment also provided useful information of the triplet excited state of the examined samples. The registered fluorescence spectra for the monomers **3a–c**, **5a–c** and **6a–c** in TOL are reported in Fig. 5 and S5 (ESI section†) and the derived parameters are collected in Table 2. The monomers maintained the spectral features of the fluorescence observed at room temperature, but their maxima underwent slight hypsochromic shifts. Fluorescence lifetimes of a few nanoseconds, almost identical to those at room temperature, were measured. Intense and structured phosphorescence spectra were recorded between 450 and 650 nm when delayed spectra were registered (see the Experimental section for details) Fig. 5, S5† and Table 2. The phosphorescence lifetime was of the order of seconds, see the ESI section, Fig. S6.†

In some cases, (**5a**, **3c**, **5c**, **6c** *etc.*), delayed fluorescence was also detected, with an identical spectral shape to normal fluorescence, but a much longer lifetime. We ascribed the delayed fluorescence as a P-type, based on the lifetime. P-type delayed fluorescence is the product of a triplet–triplet reaction and, as such, its lifetime is half of that of phosphorescence, Fig. S6.†

At 77 K, the bis-imidazo[1,2-*a*]pyridines displayed a fluorescence either more resolved than at room temperature or with a slight hypsochromic shift. The delayed spectra indicated no clear trace of phosphorescence (data not shown). This result was expected since the triplet yield formation in bis-imidazo[1,2-*a*]pyridines is very low due to the extremely high radiative decay of the singlet excited state, $k_{rad} > 10^8\ s^{-1}$. Therefore, in order to detect the phosphorescence and unambiguously derive the triplet energy level, we utilized the heavy atom effect with 50% ethyl iodide (EtI), which enhances spin–orbit coupling and hence increases the triplet yield (Fig. 6 and S7†). With the addition of EtI, well-defined structured phosphorescence spectra above 550 nm were recorded. The relevant photophysical parameters are presented in Table 2. Notably, the presence of EtI not only enhanced the excited singlet to excited triplet conversion, but also helped the transition of the excited triplet to the ground state singlet. Hence, the phosphorescence lifetimes in the presence of EtI do not represent the normal triplet lifetimes and therefore, for these cases, the triplet lifetimes of the bis-imidazo[1,2-*a*]pyridines are not reported in Table 2. Again, as observed for the monomers, a delayed fluorescence was detected in almost all dimers. The 77 K experiments in DCM solutions produced results identical to those reported for TOL (data not shown).

Table 2 Photophysical parameters in TOL measured at 77 K. Delayed luminescence maxima of bis-imidazo[1,2-*a*]pyridines derived from spectra in TOL with 50% EtI. Monomers are in italics

TOL	State	λ_{em}^{max}/nm	τ/ns	E/eV[a]
3a	^{1}3a	381	5.50	3.25
	^{3}3a	469; 500; 527	0.98×10^9	2.64
5a	^{1}5a	395; 422; 452	3.61	3.14
	^{3}5a	479; 509; 549	1.08×10^9	2.59
6a	^{1}6a	394	3.10	3.14
	^{3}6a	469; 500; 540	1.31×10^9	2.64
10a	^{1}10a	455; 485	2.36	2.72
	^{3}10a	612; 669	—	2.02
3b	^{1}3b	366; 384; 404	2.58	3.38
	^{3}3b	476; 508; 541	1.02×10^9	2.60
5b	^{1}5b	391; 413; 432	4.08	3.17
	^{3}5b	479; 511; 550	1.09×10^9	2.59
6b	^{1}6b	381; 400; 420	4.27	3.25
	^{3}6b	476; 505; 538	1.29×10^9	2.60
8b	^{1}8b	492; 524	2.30	2.52
	^{3}8b	554; 595; 638	—	2.23
10b	^{1}10b	473; 504	1.42	2.62
	^{3}10b	585; 626; 680	—	2.12
3c	^{1}3c	367; 385; 404	2.31	3.37
	^{3}3c	476; 507; 533	0.85×10^9	2.60
5c	^{1}5c	394; 418; 442	3.40	3.14
	^{3}5c	481; 510; 549	0.96×10^9	2.57
6c	^{1}6c	381; 401; 424	3.65	3.25
	^{3}6c	467; 501; 543	1.11×10^9	2.65
8c	^{1}8c	509; 541	2.60	2.43
	^{3}8c	592; 650; 707	—	2.09
10c	^{1}10c	487; 517	1.70	2.54
	^{3}10c	553; 592; 635	—	2.24

[a] E_{0-0} from the maxima of the luminescence spectra at 77 K.

Two-photon absorption

The two-photon absorption (2PA) cross-sections of bis-imidazo[1,2-*a*]pyridines **8b,c** and **10a–c** were determined in solution

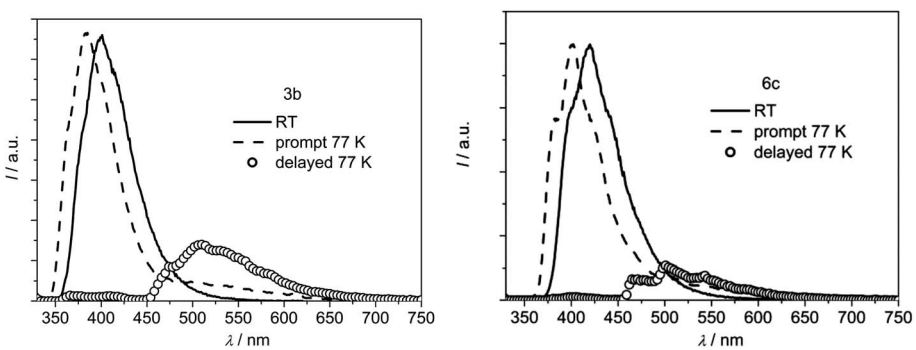

Fig. 5 Prompt and delayed luminescence of **3b** and **6c** in TOL at room temperature and 77 K, upon excitation at 325 nm. The scale of luminescence intensity is arbitrary. Other data can be found in the ESI section.†

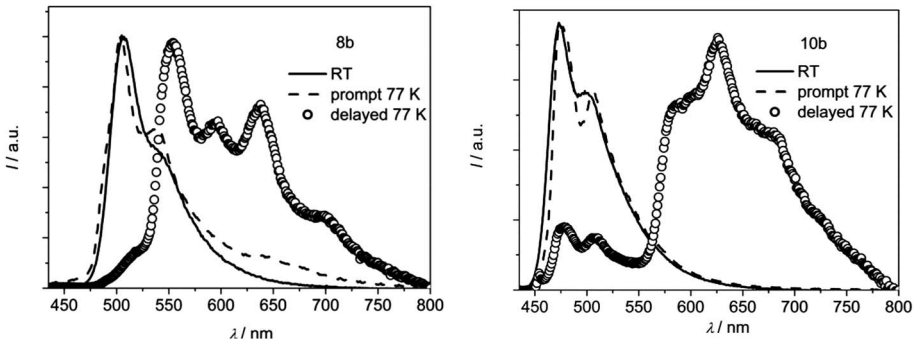

Fig. 6 RT luminescence in TOL and prompt and delayed luminescence at 77 K of **8b** and **10b** in TOL with 50% EtI, upon excitation at 424 nm. The scale of luminescence intensity is arbitrary. Other data can be found in the ESI section.†

using the two-photon induced fluorescence (TPE) methodology.[18] The measurements were conducted in the 700–1000 nm range (corresponding to the relevant biological spectral window) (Table 3). As illustrated in Fig. 7 for compound **8b**, the lowest (strongly one-photon allowed) excited state is almost silent, a higher (only weakly one-photon allowed) state is responsible for the large 2PA response. This feature, common to all bis-imidazo[1,2-*a*]pyridines compounds **8b,c** and **10a–c** (Fig. S8, ESI section†), was consistent with the behavior of symmetrical quadrupolar derivatives.[1f,19]

Dimeric symmetrical compounds **8b,c** constructed from a (electron-withdrawing) dicyanobenzene core exhibited an intense 2PA band located around 800 nm (Fig. 8). The 2PA maxima were almost unaffected by the presence of the solubilizing OTEG side chains on the phenyl substituents of the imidazo[1,2-*a*]pyridine terminal moieties whereas a red-shift of the 2PA band was observed (30 nm). These factors contributed

Table 3 Two-photon absorption properties of bis-imidazo[1,2-*a*]-pyridines in DCM

	$2\lambda_{OPA}^{max}$/nm	λ_{TPA}^{max}/nm	σ_2^{max}/GM	$\sigma_2^{max}\phi_{fl}$/GM
8b	942, 748	770	880	730
8c	968, 762	800	800	640
10a	848	≤700	≥500	>180
10b	880	730	640	560
10c	900, 620	750	550	450

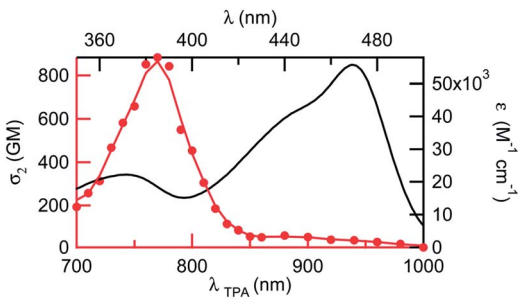

Fig. 7 Two-photon absorption spectra of bis-imidazo[1,2-*a*]pyridine **8b** (full circles) compared to rescaled one-photon absorption spectra (solid line).

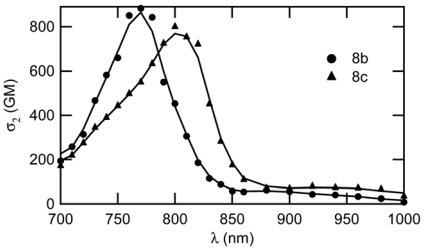

Fig. 8 Two-photon absorption spectra of bis-imidazo[1,2-*a*]pyridines **8b,c**.

to a maximum 2PA cross-section of about 800 GM at 800 nm, resulting in a large two-photon brightness ($\sigma_2\phi_{fl}$ = 640 GM) for the unconventional symmetrical "quadrupolar-like" derivative **8c**.

Related dimeric symmetrical compounds **10a–c** constructed from a pyrazine core showed an intense 2PA band located in the 700–750 nm spectral region (Fig. 9). As observed with compounds **8b,c**, the nature of the substituents on the imidazo[1,2-*a*]pyridine terminal moieties affected the position of the 2PA band (as the electron donating strength increased, the peak became more red shifted) whereas the peak 2PA cross-sections were similar with a two-photon absorption maximum cross-section in the 550–650 GM range, resulting in two-photon brightness values of 450–550 GM (Table 3). Comparison of the 2PA responses of derivatives **8b,c** and **10b,c** indicated that the dicyanobenzene-core derivatives displayed 2PA bands that were more intense and more red-shifted (allowing deeper

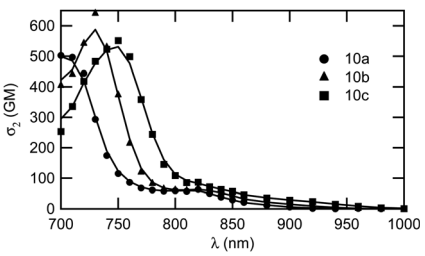

Fig. 9 Two-photon absorption spectra of bis-imidazo[1,2-*a*]pyridines **10a–c**.

penetration depth in scattering media) than their pyrazine-cored analogues. However, the hydrophilic pyrazine core structures may prove more promising for bioimaging purposes. The poor solubility of the OTEG substituted samples in water prevents the 2PA absorption spectra determination. However, taking into account the fluorescence quantum yield, a two-photon brightness of about 80 GM can be estimated for the hydrophilic two-photon dye **10c** in this solvent, whereas compound **8c** shows a two-photon brightness of about 30 GM.

When compared with other D–A–D systems possessing a 1,4-dicyanobenzene core,[20] dyes **8b,c** exhibited comparably high fluorescence quantum yields but higher two-photon absorption cross-section values. They also showed bathochromically shifted emission. Since the pyrazine core had never been utilized before in the construction of two-photon active dyes, no direct comparisons of the optical behavior of compounds **10a–c** were possible. Still, they compare very favorably with quadrupolar dyes of similar complexity[1i,m,o] and are expected to be more biocompatible.

Conclusions

We have provided a synthesis route for intensely emitting two-photon fluorophores and discovered that by utilizing the electron-rich nature of imidazo[1,2-*a*]pyridines, it is possible to obtain a π-expanded ring system with superb two-photon brightness. The π-expansion of the imidazo[1,2-*a*]pyridine skeleton at position C3 increased the fluorescence quantum yield from <0.2 to ~1.0. These D–A–D type bis-imidazo[1,2-*a*]-pyridines are characterized by high absorbance in the visible region (400–550 nm) with a molar absorption coefficient of 5×10^4 M^{-1} cm^{-1} and intense fluorescence in the wavelength range 450–600 nm. In addition, the bis-imidazo[1,2-*a*]pyridines showed significant 2PA responses in the biological spectral window. The dimers with the dicyanobenzene-core showed red-shifted and enhanced 2PA bands as compared to their pyrazine-core analogues. Linking two imidazo[1,2-*a*]pyridine moieties at position C3 offers significant advantages over similar D–A–D architectures linked at position C5.[3] In particular, the fluorescence quantum yield is 2.5 times higher and the σ_2 is ~10 times larger, permitting these quadrupolar compounds to display significant two-photon brightness (500–750 GM). Among these compounds, the dye which combines a hydrophilic core (pyrazine) and substituents (OTEG) holds great promise as a two-photon probe for bioimaging.

Experimental section

General

Materials. All commercially available compounds were used as received. All solvents were dried and distilled prior to use. Transformations and handling of oxygen sensitive compounds were performed under an argon atmosphere. The reaction progress was monitored by means of thin layer chromatography (TLC) which was performed on aluminium sheets, coated with silica gel 60 F_{254} (Merck) or aluminium oxide 60 F_{254} (neutral Merck) with detection by use of a UV-lamp. Product purification was done by means of column chromatography with silica flash P60 (40–63 μm, SiliCycle) or aluminum oxide 90 (neutral, 70–230 mesh, Merck), and dry column vacuum chromatography (DCVC) with silica (MN-Kieselgel P/UV_{254}) or aluminum oxide (MN-aluminiumoxid G).

Identity and purity of prepared compounds. Compound structures were proved by ^1H NMR and ^{13}C NMR (Varian 500/200 MHz). High-resolution mass spectra (EI HRMS, ESI HRMS, and FD HRMS) were obtained on a MaldiSYNAPT G2-S HDMS/GCT Premier, Waters. All melting points were measured with an Ez-Melt, SRS and were given without correction.

Synthesis

1-(4-(2-(2-(2-Methoxyethoxy)ethoxy)ethoxy)phenyl)ethanone (2c). 1-(4-(2-(2-(2-Methoxyethoxy)ethoxy)ethoxy)phenyl)ethanone (**2c**) was synthesized *via* a typical protection procedure from 4′-hydroxyacetophenone. Most of the product was recrystallized from hexane : EtOAc prior to use for analysis, except for bis-imidazopyridines (recrystallized or isolated by trituration with $CHCl_3$).

2-Methyl-6-(trifluoromethyl)imidazo[1,2-*a*]pyridine (3a). A mixture of 2-amino-5-(trifluoromethyl)pyridine **1** (3.9 g, 24 mmol) and chloroacetone (1.7 mL, 20 mmol) in ethanol (20 mL) was heated under reflux for 48 h. The ethanol was removed by evaporation to obtain a yellow oil. 5% $Na_2CO_{3(aq)}$ was then added to the residual material, followed by direct extraction with water and dichloromethane. The oil was dried under reduced pressure and cooled to obtain crystals which were then recrystallized from hexane to afford **3a** (0.89 g, 22%) as a off-white crystal, mp. 112.5 °C. ^1H NMR (500 MHz, $CDCl_3$): δ 8.40 (d, $J = 1$ Hz, 1H), 7.59 (d, $J = 9.0$ Hz, 1H), 7.43 (s, 1H), 7.26 (dd, $J_1 = 9.5$ Hz, $J_2 = 1.5$ Hz, 1H), 2.48 (s, 3H). Physicochemical properties concur with existing data.[21]

Other imidazo[1,2-*a*]pyridine derivatives were prepared *via* the Ortoleva–King–Chichibabin procedure[7a] with slight modifications.

2-Phenyl-6-(trifluoromethyl)imidazo[1,2-*a*]pyridine (3b). A round-bottom pressure flask (250 mL) charged with **1** (1.6 g, 10 mmol), acetophenone (0.6 mL, 5 mmol), and I_2 (2.0 g, 8 mmol) was heated at 100 °C for 19 h. $NaOH_{(aq)}$ (50%, 50 mL) was then added and the mixture was refluxed for 1.5 h (the mixture must be homogeneous). After cooling to r.t. the mixture was dissolved in CH_2Cl_2 and subsequently 300 mL H_2O was added and the mixture was extracted with CH_2Cl_2. The organic phase was dried over anhydrous Na_2SO_4, filtered, and the solvent was removed. The extract was used without further purification (purity proved by NMR) and afforded **3b** (1.17 g, 89%), as an off-white crystal, mp. 192.5 °C. ^1H NMR (200 MHz, $CDCl_3$): δ 8.48 (m, 1H), 7.98–7.93 (m, 3H), 7.72 (dd, $J_1 = 8$ Hz, $J_2 = 1.5$ Hz, 1H), 7.50–7.29 (m, 4H).

2-(4-(2-(2-(2-Methoxyethoxy)ethoxy)ethoxy)phenyl)-6-(trifluoromethyl)imidazo[1,2-*a*]pyridine (3c). Prepared following the procedure for **3b** from 1-(4-(2-(2-(2-methoxyethoxy)ethoxy)ethoxy)phenyl)ethanone **2c** (2.82 g, 10 mmol). The mixture was purified by DCVC on SiO_2 ($CHCl_3$) to afford **3c** (1.88 g, 44%), as an off-white amorphous solid, mp. 68–70 °C. ^1H NMR (500 MHz, $CDCl_3$): δ 8.47 (s, 1H), 7.88–7.85 (m, 3H), 7.68 (d, $J = 9.5$ Hz, 1H),

7.29 (dd, $J_1 = 9$ Hz, $J_2 = 2$ Hz, 1H), 7.01–6.98 (m, 2H), 4.18 (t, $J = 5$ Hz, 2H), 3.88 (t, $J = 5$ Hz, 2H), 3.75 (m, 2H), 3.69 (m, 2H), 3.66 (m, 2H), 3.55 (m, 2H), 3.37 (s, 3H). ^{13}C NMR (126 MHz, $CDCl_3$) δ 159.4, 147.8, 145.4, 127.6, 125.9, 124.5, 124.5, 120.5, 117.9, 115.1, 108.4, 72.1, 71.0, 70.8, 70.7, 69.9, 67.6, 59.2; HRMS (ESI): m/z ($[M + H]^+$) calcd for $C_{21}H_{23}F_3N_2O_4$: 425.1688; found: 425.1685.

3-Bromo-2-methyl-6-(trifluoromethyl)imidazo[1,2-*a*]pyridine (4a). NBS (0.53 g, 3 mmol) was added to **3a** (0.6 g, 3 mmol) in dry acetonitrile (1 mL). The mixture was stirred for 1 h at r.t., and the resulting solid was filtered, dried, and used without further purification to afford **4a** (0.69 g, 83%), as an off-white amorphous solid, mp. 86 °C. ^{1}H NMR (500 MHz, $CDCl_3$): δ 8.39 (dd, $J_1 = 1$ Hz, $J_2 = 2$ Hz, 1H), 7.63 (d, $J_1 = 9.5$ Hz, $J_2 = 1$ Hz, 1H), 7.35 (dd, $J_1 = 9.5$ Hz, $J_2 = 1.5$ Hz, 1H), 7.28 (d, $J = 7.0$ Hz, 1H), 2.49 (s, 3H). ^{13}C NMR (126 MHz, $CDCl_3$) δ 145.1, 144.4, 122.8, 122.8, 120.4, 117.8, 95.0, 13.8; HRMS (EI): m/z (M^+) calcd for $C_9H_6BrF_3N_2$: 277.9666; found: 277.9665.

3-Bromo-2-phenyl-6-(trifluoromethyl)imidazo[1,2-*a*]pyridine (4b). 3-Bromo-2-phenyl-6-(trifluoromethyl)imidazo[1,2-*a*]pyridine (**4b**) was prepared following the procedure for **4a**. Compound **3b** (1.57 g, 6 mmol) afforded **4b** (1.69 g, 82%) as an off-white amorphous solid, mp. 154 °C. ^{1}H NMR (500 MHz, $CDCl_3$): δ 8.55 (s, 1H), 8.14–8.13 (m, 2H), 7.75 (d, $J = 9.5$ Hz, 1H), 7.52–7.49 (m, 2H), 7.45–7.41 (m, 2H). ^{13}C NMR (126 MHz, $CDCl_3$) δ 145.4, 144.8, 132.2, 129.0, 128.8, 128.1, 123.3, 123.2, 121.2, 118.5, 117.9, 117.6, 93.5; HRMS (EI): m/z (M^+) calcd for $C_{14}H_8F_3N_2$: 339.9823; found: 339.9830.

3-Bromo-2-(4-(2-(2-(2-methoxyethoxy)ethoxy)ethoxy)phenyl)-6-(trifluoromethyl)imidazo[1,2-*a*]pyridine (4c). 3-Bromo-2-(4-(2-(2-(2-methoxyethoxy)ethoxy)ethoxy)phenyl)-6-(trifluoromethyl)-imidazo[1,2-*a*]pyridine (**4c**) was prepared following the procedure for **4a**. Compound **3c** (1.06 g, 2.5 mmol) afforded **4c** (1.09 g, 86%) as an off-white amorphous solid, mp. 125–126 °C. ^{1}H NMR (500 MHz, $CDCl_3$): δ 8.52 (s, 1H), 8.01 (d, $J = 9$ Hz, 2H), 7.71 (d, $J = 9.5$ Hz, 1H), 7.40 (d, $J = 9$ Hz, 1H), 7.04 (d, $J = 8.5$ Hz, 2H), 4.20 (s, 2H), 3.95 (s, 2H), 3.76 (m, 2H), 3.70 (m, 2H), 3.66 (m, 2H), 3.55 (s, 2H), 3.38 (s, 3H). ^{13}C NMR (126 MHz, $CDCl_3$) δ 159.5, 145.3, 144.6, 129.6, 124.9, 123.1, 121.0, 118.2, 117.4, 114.9, 92.7, 72.1, 71.0, 70.8, 70.7, 69.8, 67.6, 59.2; HRMS (ESI): m/z ($[M + H]^+$) calcd for $C_{21}H_{24}BrF_3N_2O_4$: 504.0793; found: 504.0794.

General procedure for the synthesis of 4-(imidazo[1,2-*a*]-pyridin-3-yl)-2-methylbut-3-yn-2-ols (alkynols)

$Pd(PPh_3)_2Cl_2$ (28 mg, 4 mol%) was added to the mixture of bromo-imidazopyridine (1 mmol) and 2-methylbut-3-yn-2-ol (0.2 mL, 2 mmol) in DMF_{anh} (3 mL) and TEA_{anh} (10 mL) under a continuous flow of argon. After bubbling through with argon for 10–30 minutes, CuI (10 mg, 5 mol%) was added and the mixture was heated at 80 °C for 17 hours. Upon completion, the resulting mixture was evaporated under reduced pressure with celite/silica and purified as follows.

2-Methyl-4-(2-methyl-6-(trifluoromethyl)imidazo[1,2-*a*]pyridin-3-yl)but-3-yn-2-ol (5a). Compound **4a** (0.56 g, 2 mmol), purified by DCVC on neutral aluminium oxide (1% MeOH in CH_2Cl_2) afforded **5a** (0.42 g, 74%), as colorless crystals, mp. 140–142 °C. ^{1}H NMR (500 MHz, $CDCl_3$): δ 8.42 (s, 1H), 7.65 (d, $J = 9$ Hz, 1H), 7.33 (dd, $J_1 = 9$ Hz, $J_2 = 2$ Hz, 1H), 2.52 (s, 3H), 1.72 (s, 6H). ^{13}C NMR (126 MHz, $CDCl_3$) δ 123.7, 121.4, 117.6, 107.0, 66.1, 31.7, 14.3; HRMS (EI): m/z (M^+) calcd for $C_{14}H_{13}F_3N_2O$: 282.0980; found: 282.0981.

2-Methyl-4-(2-phenyl-6-(trifluoromethyl)imidazo[1,2-*a*]pyridin-3-yl)but-3-yn-2-ol (5b). Compound **4b** (1.36 g, 4 mmol), purified by DCVC on SiO_2 (1% MeOH in CH_2Cl_2) afforded **5b** (1.26 g, 91%), as colorless crystals, mp. 120–121 °C. ^{1}H NMR (500 MHz, $CDCl_3$): δ 8.43 (s, 1H), 8.23–8.21 (m, 2H), 7.73 (d, $J = 9$ Hz, 1H), 7.43–7.35 (m, 4H). ^{13}C NMR (126 MHz, $CDCl_3$) δ 149.9, 144.7, 132.6, 129.3, 128.6, 127.3, 123.9, 123.9, 122.2, 118.1, 107.5, 70.6, 66.1, 31.5; HRMS (EI): m/z (M^+) calcd for $C_{19}H_{15}F_3N_2O$: 344.1136; found: 344.1138.

4-(2-(4-(2-(2-(2-Methoxyethoxy)ethoxy)ethoxy)phenyl)-6-(trifluoromethyl)imidazo[1,2-*a*]pyridin-3-yl)-2-methylbut-3-yn-2-ol (5c). Compound **4c** (0.76 g, 1.5 mmol), purified by DCVC on SiO_2 (75% Et_2O in hexanes) afforded **5c** (0.75 g, 99%), as colorless crystals, mp. 78–79 °C. ^{1}H NMR (500 MHz, $CDCl_3$): δ 8.46 (d, $J = 1$ Hz, 1H), 8.19–8.17 (m, 2H), 7.69 (d, $J = 9$ Hz, 1H), 7.36 (dd, $J_1 = 9.5$ Hz, $J_2 = 1.5$ Hz, 1H), 6.99–6.96 (m, 2H), 4.18 (t, $J = 5$ Hz, 2H), 3.88 (t, $J = 5$ Hz, 2H), 3.75 (m, 2H), 3.69 (m, 2H), 3.66 (m, 2H), 3.55 (m, 2H), 3.38 (s, 3H), 1.74 (s, 6H). ^{13}C NMR (126 MHz, $CDCl_3$) δ 159.7, 149.6, 144.7, 128.7, 125.5, 123.8, 123.7, 122.0, 117.8, 114.7, 107.4, 72.1, 71.0, 70.8, 70.7, 69.8, 67.6, 66.1, 59.2, 31.5; HRMS (ESI): m/z ($[M + H]^+$) calcd for $C_{26}H_{30}F_3N_2O_5$: 507.2107; found: 507.2108.

General procedure for the synthesis of 3-ethynylimidazo[1,2-*a*]-pyridine

A solution of alkynol (1 mmol) and NaOH (30 mg) in $toluene_{anh}$ (2 mL) was heated at 120 °C under argon in an ACE pressure tube for 2 h. Then the mixture was evaporated with silica and purified as follows:

3-Ethynyl-2-methyl-6-(trifluoromethyl)imidazo[1,2-*a*]pyridine (6a). Compound **5a** (283 mg, 1 mmol) and KOH (60 mg, 1.1 mmol) instead of NaOH, purified by DCVC on neutral aluminium oxide (1% MeOH in CH_2Cl_2) afforded **6a** (145 mg, 65%), as colorless crystals, mp. 109.5 °C. ^{1}H NMR (500 MHz, $CDCl_3$): δ 8.54 (s, 1H), 7.64 (d, $J = 9$ Hz, 1H), 7.38 (dd, $J_1 = 9$ Hz, $J_2 = 1.5$ Hz, 1H), 3.97 (s, 1H), 2.52 (s, 3H). ^{13}C NMR (126 MHz, $CDCl_3$) δ 151.4, 144.6, 124.0, 124.0, 121.7, 117.7, 90.3, 70.9, 14.5; HRMS (EI): m/z (M^+) calcd for $C_{11}H_7F_3N_2$: 224.0561; found: 224.0566.

3-Ethynyl-2-phenyl-6-(trifluoromethyl)imidazo[1,2-*a*]pyridine (6b). Compound **5b** (345 mg, 1 mmol), purified by DCVC on SiO_2 (CH_2Cl_2) (228 mg, 79%) afforded **6b**, as colorless crystals, mp. 160 °C. ^{1}H NMR (500 MHz, $CDCl_3$): δ 8.65 (m, 1H), 8.32–8.30 (m, 2H), 7.75 (d, $J = 9.5$ Hz, 1H), 7.51–7.42 (m, 4H). ^{13}C NMR (126 MHz, $CDCl_3$) δ 150.5, 144.9, 132.5, 129.4, 128.8, 127.5, 124.3, 124.2, 122.5, 118.3, 91.2, 72.3; HRMS (EI): m/z (M^+) calcd for $C_{16}H_9F_3N_2$: 286.0718; found: 286.0726.

3-Ethynyl-2-(4-(2-(2-(2-methoxyethoxy)ethoxy)ethoxy)phenyl)-6-(trifluoromethyl)imidazo[1,2-*a*]pyridine (6c). Compound **5c** (634 mg, 1.25 mmol), purified by DCVC on SiO_2 (1% MeOH in $CHCl_3$) afforded **6c** (399 mg, 71%), as colorless crystals, mp.

136.5–137 °C. ^{1}H NMR (500 MHz, $CDCl_3$): δ 8.62 (s, 1H), 8.26–8.24 (m, 2H), 7.72 (d, $J = 9.5$ Hz, 1H), 7.42 (dd, $J_1 = 8$ Hz, $J_2 = 2$ Hz, 1H), 7.04–7.02 (m, 2H), 4.21 (t, $J = 5$ Hz, 2H), 4.14 (s, 1H), 3.89 (t, $J = 5$ Hz, 2H), 3.76 (m, 2H), 3.70 (m, 2H), 3.67 (m, 2H), 3.55 (m, 2H), 3.38 (s, 3H). ^{13}C NMR (126 MHz, $CDCl_3$) δ 159.9, 150.5, 144.9, 128.9, 125.4, 124.1, 124.1, 122.3, 117.9, 114.9, 104.3, 91.1, 72.6, 72.1, 71.0, 70.8, 70.7, 69.8, 67.6, 59.2; HRMS (ESI): m/z ($[M + H]^+$) calcd for $C_{23}H_{24}F_3N_2O_4$: 449.1688; found: 449.1685.

General procedure for the synthesis of bis-imidazo[1,2-*a*]-pyridines

$Pd(PPh_3)_2Cl_2$ (28 mg, 4 mol%) was added to a mixture of the corresponding alkyne (1 mmol), dihaloarene (0.5 mmol), in anhydrous DMF and anhydrous TEA under a continuous flow of argon gas in a Schlenk flask. The resulting mixture was bubbled through with argon gas for 30 min, closed, and heated. Then, the mixture was evaporated with Celite and purified as follows:

2,5-Bis((2-phenyl-6-(trifluoromethyl)imidazo[1,2-*a*]pyridin-3-yl)ethynyl)terephthalonitrile (8b). Compound **6b** (172 mg, 0.6 mmol) and 2,5-dibromoterephthalonitrile (83 mg, 0.29 mmol) in 8 mL of DMF : TEA (1 : 3) were heated at 50 °C for 4 h. The mixture was purified by DCVC on silica (1% MeOH in $CHCl_3$) to afford **8b** (151 mg, 75%), as an orange amorphous solid; the compound decomposed at 280 °C. ^{1}H NMR (500 MHz, TFA): δ 9.27 (s, 2H), 8.39 (d, $J = 9$ Hz, 2H), 8.34 (s, 2H), 8.28 (d, $J = 9$ Hz, 2H), 8.17 (d, $J = 6.5$ Hz, 4H), 7.71–7.66 (m, 6H). ^{13}C NMR (126 MHz, $CDCl_3$) δ 144.8, 142.4, 138.5, 135.4, 134.4, 131.9, 129.7, 128.2, 125.4, 108.3, 99.2, 88.8; HRMS (EI): m/z (M^+) calcd for $C_{40}H_{18}F_6N_6$: 696.1497; found: 696.1507.

2,5-Bis((2-(4-(2-(2-(2-methoxyethoxy)ethoxy)ethoxy)phenyl)-6-(trifluoromethyl)imidazo[1,2-*a*]pyridin-3-yl)ethynyl)terephthalonitrile (8c). Compound **6c** (68 mg, 0.15 mmol) and 2,5-dibromoterephthalonitrile 7 (21.5 mg, 0.075 mmol) in 1.5 mL of TEA were heated at 80 °C for 4.5 h. The mixture was purified by DCVC on silica (1% MeOH in $CHCl_3$) to afford **8c** (20 mg, 26%), as an orange amorphous solid; the compound decomposed at 260 °C. ^{1}H NMR (500 MHz, $CDCl_3$): δ 8.91 (s, 2H), 8.30–8.27 (m, 4H), 7.94 (s, 2H), 7.78 (d, $J = 9$ Hz, 2H), 7.53 (dd, $J_1 = 9.5$ Hz, $J_2 = 2$ Hz, 2H), 7.11–7.09 (m, 4H), 4.25 (t, $J = 5$ Hz, 4H), 3.92 (s, 4H), 3.78 (m, 4H), 3.71 (m, 4H), 3.68 (m, 4H), 3.57 (m, 4H), 3.38 (s, 6H). ^{13}C NMR (126 MHz, $CDCl_3$) δ 160.5, 152.9, 146.3, 134.7, 129.3, 125.8, 124.9, 124.7, 123.8, 118.2, 117.5, 116.3, 115.2, 103.8, 97.9, 89.5, 72.1, 71.1, 70.8, 70.7, 69.8, 67.8, 59.2; HRMS (ESI): m/z ($[M + Na]^+$) calcd for $C_{54}H_{46}F_6N_6O_8Na$: 1043.3179; found: 1043.3180.

2,5-Bis((2-methyl-6-(trifluoromethyl)imidazo[1,2-*a*]pyridin-3-yl)ethynyl)pyrazine (10a). Compound **6a** (34 mg, 0.15 mmol) and 2-bromo-5-iodopyrazine (**9**, 21.4 mg, 0.075 mmol) in 1.5 mL of TEA were heated at 50 °C for 16 h. The mixture was purified by flash chromatography ($CHCl_3$) to afford **10a** (30 mg, 77%), as a yellow amorphous solid; the compound decomposed at 295 °C. ^{1}H NMR (500 MHz, $CDCl_3$): δ 8.82 (s, 2H), 8.67 (s, 2H), 7.71 (d, $J = 9.5$ Hz, 2H), 7.47 (d, $J = 9$ Hz, 2H), 2.68 (s, 6H). ^{13}C NMR (126 MHz, $CDCl_3$) δ 153.4, 146.8, 145.6, 137.5, 124.3, 122.7, 118.2, 118.0, 106.8, 99.4, 82.2, 14.9; HRMS (EI): m/z (M^+) calcd for $C_{26}H_{14}F_6N_6$: 524.1184; found 524.1187.

2,5-Bis((2-phenyl-6-(trifluoromethyl)imidazo[1,2-*a*]pyridin-3-yl)-ethynyl)pyrazine (10b). Compound **6b** (43 mg, 0.15 mmol) and 2-bromo-5-iodopyrazine **9** (21.4 mg, 0.075 mmol) in 1.5 mL of TEA were heated at 80 °C for 16 h. The mixture was purified by DCVC on silica ($CHCl_3$) to afford **10b** (30 mg, 56%), as a yellow amorphous solid; the compound decomposed at 315 °C. ^{1}H NMR (500 MHz, TFA): δ 9.42 (s, 2H), 9.39 (s, 2H), 8.46 (d, $J = 9$ Hz, 2H), 8.41 (d, $J = 9$ Hz, 2H), 8.23 (dd, $J_1 = 8$ Hz, $J_2 = 1$ Hz, 4H), 7.88–7.83 (m, 6H). ^{13}C NMR (126 MHz, $CDCl_3$) δ 147.0, 143.5, 140.3, 136.4, 133.4, 132.7, 129.9, 127.4, 123.1, 113.6, 106.0, 97.0, 81.4; HRMS (ESI): m/z ($[M + H]^+$) calcd for $C_{36}H_{19}F_6N_6$: 649.1575; found: 649.1581.

2,5-Bis((2-(4-(2-(2-(2-methoxyethoxy)ethoxy)ethoxy)phenyl)-6-(trifluoromethyl)imidazo[1,2-*a*]pyridin-3-yl)ethynyl)pyrazine (10c). Compound **6c** (68 mg, 0.15 mmol) and 2-bromo-5-iodopyrazine **9** (21.4 mg, 0.075 mmol) in 1.5 mL of TEA were heated at 80 °C for 4.5 h. The mixture was purified by DCVC on silica ($CHCl_3$) to afford **10c** (37 mg, 51%), as a yellow amorphous solid; the compound decomposed at 246 °C. ^{1}H NMR (500 MHz, $CDCl_3$): δ 8.84 (s, 2H), 8.74 (s, 2H), 8.31–8.29 (m, 4H), 7.78 (d, $J = 9$ Hz, 2H), 7.50 (dd, $J_1 = 9$ Hz, $J_2 = 2$ Hz, 2H), 7.09–7.07 (m, 4H), 4.23 (t, $J = 5$ Hz, 4H), 3.91 (s, 4H), 3.77 (m, 4H), 3.71 (m, 4H), 3.67 (m, 4H), 3.56 (m, 4H), 3.38 (s, 6H). ^{13}C NMR (126 MHz, $CDCl_3$) δ 160.3, 152.4, 146.9, 145.9, 137.5, 129.2, 125.2, 124.4, 124.4, 123.3, 122.4, 118.3, 117.9, 104.0, 99.9, 84.1, 72.1, 71.1, 70.8, 70.7, 69.8, 67.7, 59.2; HRMS (ESI): m/z ($[M + Na]^+$) calcd for $C_{50}H_{46}F_6N_6O_8Na$: 995.3179; found: 995.3187.

Photophysics

The solvents used were spectroscopic grade toluene and dichloromethane (C. Erba). All samples were freshly prepared and carefully stored in the dark before the experiments. Ethyl iodide was from Aldrich. Absorption spectra were recorded with a Perkin-Elmer Lambda 650 spectrophotometer and the emission spectra, corrected for the photomultiplier (PMT) response if not otherwise stated, were detected by using an Edinburgh FLSP920 fluorometer equipped with a R928P Hamamatsu photomultiplier. Luminescence quantum yields of the samples, ϕ_s, were evaluated against a standard with known emission quantum yield ϕ_r by comparing areas under the corrected luminescence spectra by using the equation: $\phi_s/\phi_r = A_r n_s^2 (\text{area})_s / A_s n_r^2 (\text{area})_r$, where A is the absorbance, n is the refractive index of the solvent employed and s and r stand for the sample and reference, respectively. The standard used for monomers was air-equilibrated quinine sulfate in 1 N H_2SO_4 with an emission quantum yield $\phi_{fl} = 0.546$,[22] whereas for bis-imidazo[1,2-*a*]pyridines, air-equilibrated coumarin 153 in ethanol with an emission quantum yield $\phi_{fl} = 0.544$ was used.[23] Determinations at 77 K on glassy solutions made use of capillary quartz tubes dipped in a home-made quartz Dewar filled with liquid nitrogen and made use of the same Edinburg FLSP920 apparatus. Phosphorescence spectra, corrected for the PMT response, were registered upon excitation with a microsecond Xenon flash lamp μF920H, after a 1 ms delay and with a 50 ms gate. Phosphorescence spectra of bis-imidazo[1,2-*a*]pyridines in glassy solvents with 50% ethyl iodide were registered upon excitation with the same lamp, after a 0.550 ms delay and with a

10 ms gate. The phosphorescence lifetimes in the millisecond–second range were measured with the same instrument and elaborated with standard curve fitting software procedures. Fluorescence lifetimes in the nanosecond region were detected by using a Time Correlated Single Photon Counting apparatus (IBH) with excitation at 331 or 373 nm.

Estimated errors are 10% on molar extinction coefficients and quantum yields and 2 nm on emission and absorption maxima. The working temperature, if not otherwise specified, is 295 ± 2 K.

Two-photon absorption

Two-photon absorption cross-sections (σ_2) were determined from the two-photon fluorescence (TPEF) action cross-sections (two-photon brightness, $\sigma_2\phi_{fl}$) and the fluorescence emission quantum yield (ϕ_{fl}). TPEF action cross-sections were measured relative to fluorescein in 0.01 M aqueous NaOH in the 715–980 nm range,[18,24] using the method described by Xu and Webb and the appropriate solvent-related refractive index corrections.[25] Reference values between 700 and 715 nm for fluorescein were taken from the literature.[26] The quadratic dependence of the fluorescence intensity on the excitation power was checked at all wavelengths. Measurements were conducted using an excitation source delivering fs pulses. This procedure prevents excited-state absorption during the pulse duration, a phenomenon which has been shown to lead to overestimated two-photon absorption cross-section values. To scan the 680–1080 nm range, a Nd:YVO4-pumped Ti:sapphire oscillator was used generating 140 fs pulses at a 80 MHz rate. The excitation was focused into the cuvette through a microscope objective (10×, NA 0.25). The fluorescence was detected in epifluorescence mode *via* a dichroic mirror (Chroma 675dcxru) and a barrier filter (Chroma e650sp-2p) by a using a compact CCD spectrometer module BWTek BTC112E. Total fluorescence intensities were obtained by integrating the corrected emission. The experimental uncertainty of the two-photon action cross-section values determined from this method has been estimated to be ±10%.

Acknowledgements

LF thanks the CNR of Italy (DP.04.010, Project MACOL) and MBD gratefully acknowledges Conseil Régional d'Aquitaine for financial support (Chaire d'Accueil grant and fellowship to VH). The research leading to these results has received partial funding from the European Community's Seventh Framework Programme under TOPBIO project-grant agreement no. 264362. We thank Jillian Larsen (UC Riverside) for a preliminary reading of the text.

Notes and references

1 (*a*) W. Denk, J. H. Strickler and W. W. Webb, *Science*, 1990, **248**, 73–76; (*b*) K. Svoboda, W. Denk, D. Kleinfeld and D. W. Tank, *Nature*, 1997, **385**, 161–165; (*c*) T. R. Krishna, M. Parent, M. H. V. Werts, L. Moreaux, S. Gmouh, S. Charpak, A.-M. Caminade, J.-P. Majoral and M. Blanchard-Desce, *Angew. Chem., Int. Ed.*, 2006, **45**, 4645–4648; (*d*) H. A. Collins, M. Khurana, E. H. Moriyama, A. Mariampillai, E. Dahlstedt, M. Balaz, M. K. Kuimova, M. Drobizhev, V. X. D. Yang, D. Phillips, A. Rebane, B. C. Wilson and H. L. Anderson, *Nat. Photonics*, 2008, **2**, 420–424; (*e*) H. M. Kim and B. R. Cho, *Chem. Commun.*, 2009, 153–164; (*f*) H. M. Kim and B. R. Cho, *Chem. – Asian J.*, 2011, **6**, 58–69; (*g*) V. Parthasarathy, S. Fery-Forgues, E. Campioli, G. Recher, F. Terenziani and M. Blanchard-Desce, *Small*, 2011, **7**, 3219–3229; (*h*) H.-Y. Ahn, K. E. Fairfull-Smith, B. J. Morrow, V. Lussini, B. Kim, M. V. Bondar, S. E. Bottle and K. D. Belfield, *J. Am. Chem. Soc.*, 2012, **134**, 4721–4730; (*i*) S. K. Das, C. S. Lim, S. Y. Yang, J. H. Han and B. R. Cho, *Chem. Commun.*, 2012, **48**, 8395–8397; (*j*) J. H. Han, S. K. Park, C. S. Lim, M. K. Park, H. J. Kim, H. M. Kim and B. R. Cho, *Chem. – Eur. J.*, 2012, **18**, 15246–15249; (*k*) A. R. Morales, C. O. Yanez, Y. Zhang, X. Wang, S. Biswas, T. Urakami, M. Komatsu and K. D. Belfield, *Biomaterials*, 2012, **33**, 8477–8485; (*l*) E. W. Seo, J. H. Han, C. H. Heo, J. H. Shin, H. M. Kim and B. R. Cho, *Chem. – Eur. J.*, 2012, **18**, 12388–12394; (*m*) S. K. Bae, C. H. Heo, D. J. Choi, D. Sen, E.-H. Joe, B. R. Cho and H. M. Kim, *J. Am. Chem. Soc.*, 2013, **135**, 9915–9923; (*n*) C. Le Droumaguet, A. Sourdon, E. Genin, O. Mongin and M. Blanchard-Desce, *Chem. – Asian J.*, 2013, **8**, 2984–3001; (*o*) A. R. Morales, A. Frazer, A. W. Woodward, H.-Y. Ahn-White, A. Fonari, P. Tongwa, T. Timofeeva and K. D. Belfield, *J. Org. Chem.*, 2013, **78**, 1014–1025.

2 (*a*) M. Albota, D. Beljonne, J. L. Bredas, J. E. Ehrlich, J. Y. Fu, A. A. Heikal, S. E. Hess, T. Kogej, M. D. Levin, S. R. Marder, D. McCord-Maughon, J. W. Perry, H. Rockel, M. Rumi, C. Subramaniam, W. W. Webb, X. L. Wu and C. Xu, *Science*, 1998, **281**, 1653–1656; (*b*) B. A. Reinhardt, L. L. Brott, S. J. Clarson, A. G. Dillard, J. C. Bhatt, R. Kannan, L. X. Yuan, G. S. He and P. N. Prasad, *Chem. Mater.*, 1998, **10**, 1863–1874; (*c*) G. S. He, L.-S. Tan, Q. Zheng and P. N. Prasad, *Chem. Rev.*, 2008, **108**, 1245–1330; (*d*) F. Terenziani, C. Katan, E. Badaeva, S. Tretiak and M. Blanchard-Desce, *Adv. Mater.*, 2008, **20**, 4641–4678; (*e*) H. M. Kim and B. R. Cho, *Acc. Chem. Res.*, 2009, **42**, 863–872; (*f*) M. Pawlicki, H. A. Collins, R. G. Denning and H. L. Anderson, *Angew. Chem., Int. Ed.*, 2009, **48**, 3244–3266; (*g*) S. Yao and K. D. Belfield, *Eur. J. Org. Chem.*, 2012, 3199–3217.

3 D. Firmansyah, A. I. Ciuciu, V. Hugues, M. Blanchard-Desce, L. Flamigni and D. T. Gryko, *Chem. – Asian J.*, 2013, **8**, 1279–1294.

4 (*a*) J. Catalan, E. Mena, F. Fabero and F. Amatguerri, *J. Chem. Phys.*, 1992, **96**, 2005–2016; (*b*) A. Douhal, F. Amatguerri and A. U. Acuna, *J. Phys. Chem.*, 1995, **99**, 76–80; (*c*) H. Tomoda, T. Hirano, S. Saito, T. Mutai and K. Araki, *Bull. Chem. Soc. Jpn.*, 1999, **72**, 1327–1334; (*d*) T. Mutai, H. Tomoda, T. Ohkawa, Y. Yabe and K. Araki, *Angew. Chem., Int. Ed.*, 2008, **47**, 9522–9524; (*e*) F. Shibahara, R. Sugiura, E. Yamaguchi, A. Kitagawa and T. Murai, *J. Org. Chem.*, 2009, **74**, 3566–3568; (*f*) F. Shibahara, E. Yamaguchi, A. Kitagawa, A. Imai and T. Murai, *Tetrahedron*, 2009, **65**,

5062–5073; (*g*) H. Shono, T. Ohkawa, H. Tomoda, T. Mutai and K. Araki, *ACS Appl. Mater. Interfaces*, 2011, **3**, 654–657; (*h*) E. Yamaguchi, F. Shibahara and T. Murai, *J. Org. Chem.*, 2011, **76**, 6146–6158; (*i*) F. Shibahara, Y. Dohke and T. Murai, *J. Org. Chem.*, 2012, **77**, 5381–5388; (*j*) Y. Shigemitsu, T. Mutai, H. Houjou and K. Araki, *J. Phys. Chem. A*, 2012, **116**, 12041–12048.

5 J. Lee, J. Chung, S. M. Byun, B. M. Kim and C. Lee, *Tetrahedron*, 2013, **69**, 5660–5664.

6 (*a*) J. C. Teulade, G. Grassy, J. P. Girard, J. P. Chapat and M. Simeondebuochberg, *Eur. J. Med. Chem.*, 1978, **13**, 271–276; (*b*) E. Abignente, A. F. E. Luraschi, C. Saturnino, F. Rossi, E. Lampa, M. Cazzola, E. Brandinelli, R. Marrazzo and E. Marmo, *Rend. Atti Accad. Sci. Med. Chir.*, 1985, **139**, 313; (*c*) E. Abignente, A. F. E. Luraschi, C. Saturnino, F. Rossi, E. Lampa, M. Cazzola, E. Brandinelli, R. Marrazzo and E. Marmo, *Chem. Abstr.*, 1986, **105**, 126822z; (*d*) S. Z. Langer, S. Arbilla, J. Benavides and B. Scatton, *Adv. Biochem. Psychopharmacol.*, 1990, **46**, 61–72; (*e*) E. Abignente, *Actual. Chim. Ther.*, 1991, **18**, 193–214; (*f*) E. Abignente, *Chem. Abstr.*, 1991, **115**, 256028n; (*g*) A. Elhakmaoui, A. Gueiffier, J. C. Milhavet, Y. Blache, J. P. Chapat, O. Chavignon, J. C. Teulade, R. Snoeck, G. Andrei and E. Declercq, *Bioorg. Med. Chem. Lett.*, 1994, **4**, 1937–1940; (*h*) T. Ueda, K. Mizushige, K. Yukiiri, T. Takahashi and M. Kohno, *Cerebrovasc. Dis.*, 2003, **16**, 396–401; (*i*) K. F. Byth, J. D. Culshaw, S. Green, S. E. Oakes and A. P. Thomas, *Bioorg. Med. Chem. Lett.*, 2004, **14**, 2245–2248; (*j*) T. S. Harrison and G. M. Keating, *CNS Drugs*, 2005, **19**, 65–89; (*k*) R. B. Lacerda, C. K. F. de Lima, L. L. da Silva, N. C. Romeiro, A. L. P. Miranda, E. J. Barreiro and C. A. M. Fraga, *Bioorg. Med. Chem.*, 2009, **17**, 74–84.

7 (*a*) A. J. Stasyuk, M. Banasiewicz, M. K. Cyrański and D. T. Gryko, *J. Org. Chem.*, 2012, **77**, 5552–5558; (*b*) T. Mutai, H. Sawatani, T. Shida, H. Shono and K. Araki, *J. Org. Chem.*, 2013, **78**, 2482–2489.

8 (*a*) Y. Q. Ge, J. Jia, H. Yang, X. T. Tao and J. W. Wang, *Dyes Pigm.*, 2011, **88**, 344–349; (*b*) A. T. Khan, R. S. Basha and M. Lal, *Tetrahedron Lett.*, 2012, **53**, 2211–2217.

9 O. N. Burchak, L. Mugherli, M. Ostuni, J. J. Lacapere and M. Y. Balakirev, *J. Am. Chem. Soc.*, 2011, **133**, 10058–10061.

10 M. Leopoldo, E. Lacivita, E. Passafiume, M. Contino, N. A. Colabufo, F. Berardi and R. Perrone, *J. Med. Chem.*, 2007, **50**, 5043–5047.

11 J. Niziol, W. Baran, E. Gondek, I. V. Kityk, A. Mendys, M. Zylewski and A. H. Reshak, *Chem. Eng. Commun.*, 2009, **196**, 1466–1474.

12 (*a*) J. G. Lombardino, *J. Org. Chem.*, 1965, **30**, 2403–2407; (*b*) J. P. Paolini and R. K. Robins, *J. Org. Chem.*, 1965, **30**, 4085–4090; (*c*) W. W. Paudler, *J. Org. Chem.*, 1968, **33**, 1089–1092; (*d*) S. E. Hand and W. W. Paudler, *J. Org. Chem.*, 1980, **45**, 3738–3745; (*e*) S. Chayer, M. Schmitt, V. Collot and J. J. Bourguignon, *Tetrahedron Lett.*, 1998, **39**, 9685–9688; (*f*) D. J. Hlasta and M. J. Silbernagel, *Heterocycles*, 1998, **48**, 1015–1022; (*g*) C. Enguehard, J. L. Renou, V. Collot, M. Hervet, S. Rault and A. Gueiffier, *J. Org. Chem.*, 2000, **65**, 6572–6575; (*h*) K. Pericherla, P. Khedar, B. Khungar and A. Kumar, *Chem. Commun.*, 2013, **49**, 2924–2926.

13 Y. Nakayama, K. Hayashi and M. Irie, *Bull. Chem. Soc. Jpn.*, 1991, **64**, 202–207.

14 W. J. Youngblood, D. T. Gryko, R. K. Lammi, D. F. Bocian, D. Holten and J. S. Lindsey, *J. Org. Chem.*, 2002, **67**, 2111–2117.

15 K. Pieterse, A. Lauritsen, A. Schenning, J. Vekemans and E. W. Meijer, *Chem. – Eur. J.*, 2003, **9**, 5597–5604.

16 A. I. Ciuciu, K. Skonieczny, D. Koszelewski, D. T. Gryko and L. Flamigni, *J. Phys. Chem. C*, 2013, **117**, 791–803.

17 (*a*) F. Terenziani, A. Painelli, C. Katan, M. Charlot and M. Blanchard-Desce, *J. Am. Chem. Soc.*, 2006, **128**, 15742–15755; (*b*) C. Katan, M. Charlot, O. Mongin, C. Le Droumaguet, V. Jouikov, F. Terenziani, E. Badaeva, S. Tretiak and M. Blanchard-Desce, *J. Phys. Chem. B*, 2010, **114**, 3152–3169.

18 C. Xu and W. W. Webb, *J. Opt. Soc. Am. B*, 1996, **13**, 481–491.

19 M. Barzoukas and M. Blanchard-Desce, *J. Chem. Phys.*, 2000, **113**, 3951–3959.

20 (*a*) S. P. McIlroy, E. Clo, L. Nikolajsen, P. K. Frederiksen, C. B. Nielsen, K. V. Mikkelsen, K. V. Gothelf and P. R. Ogilby, *J. Org. Chem.*, 2005, **70**, 1134–1146; (*b*) C.-H. Zhao, A. Wakamiya, Y. Inukai and S. Yamaguchi, *J. Am. Chem. Soc.*, 2006, **128**, 15934–15935.

21 T. Fusaka, O. Ujikawa, T. Kajiwara and Y. Tanaka, *Triazole compounds, their production and use*, Takeda Chemical Industries LTD, JP, 1997, WO 1997011075 A1, p.74.

22 D. F. Eaton, *Pure Appl. Chem.*, 1988, **60**, 1107–1114.

23 K. Rurack and M. Spieles, *Anal. Chem.*, 2011, **83**, 1232–1242.

24 M. A. Albota, C. Xu and W. W. Webb, *Appl. Opt.*, 1998, **37**, 7352–7356.

25 M. H. V. Werts, N. Nerambourg, D. Pelegry, Y. Le Grand and M. Blanchard-Desce, *Photochem. Photobiol. Sci.*, 2005, **4**, 531–538.

26 C. Katan, S. Tretiak, M. H. V. Werts, A. J. Bain, R. J. Marsh, N. Leonczek, N. Nicolaou, E. Badaeva, O. Mongin and M. Blanchard-Desce, *J. Phys. Chem. B*, 2007, **111**, 9468–9483.